

Adaptive Containment Control for Nonlinear Multi-Agent Systems with Input Quantization and Sensor Faults

Wen Wen^{1,2}

¹ Three Gorges Mathematical Research Center, China Three Gorges University, Yichang, China

² College of Mathematics and Physics, China Three Gorges University, Yichang, China

Correspondence: Wen Wen, Three Gorges Mathematical Research Center, China Three Gorges University, Yichang, China; College of Mathematics and Physics, China Three Gorges University, Yichang, China

Received: April 17, 2025; Accepted: April 28, 2025; Published: April 29, 2025

Abstract

This study investigates the adaptive containment control problem for a class of nonlinear multi-agent systems with input quantization and sensor faults. A state observer and a radial basis function neural network are respectively employed to estimate unmeasurable states and approximate unknown nonlinear functions. An absolute cubic Lyapunov function is designed to compensate for the influence of sensor faults on the systems. A filter is introduced to reduce computational complexity. Adaptive laws are developed to update the estimates of uncertain dynamic parameters, fault coefficients, and the filter-error compensation term. A distributed adaptive control scheme is proposed to ensure that all followers converge to the convex hull formed by the leaders. The stability of the closed-loop system is strictly proved based on stability theory, and the effectiveness of the proposed control method is verified by numerical simulation.

Keywords: containment control, fault-tolerant control, input quantization, multi-agent systems

1. Introduction

As a core technology in distributed intelligent control, multi-agent systems (MASs) are dedicated to achieving global optimization objectives for complex tasks through local interactions and collaborative behaviors among multiple autonomous agents. Characterized by autonomy, robustness, and dynamic adaptability, MASs demonstrate significant advantages in applications such as UAV formations, traffic control, and swarm robotic coordination [1-3].

Containment control is the core branch of multi-agent system cooperative control, which aims to make the follower agents converge to the convex hull region composed of the leaders through the motion guidance of multiple leaders. With the rapid development of industrial automation and intelligent clustering technology, containment control has shown key value in dynamic target rounding, disaster relief area blocking, distributed sensor network coverage and other scenarios. In recent years, research on containment control has made remarkable progress in both theory and application [4-9]. In [10], an adaptive fuzzy tracking control problem for nonlinear systems with unmeasurable states and external disturbances was investigated. In [11], the authors studied multi-network unknown nonlinear mechanical systems and designed a distributed adaptive event-triggered sliding mode control scheme. A fixed-time feedback control strategy with integrated event triggering mechanism to solve the security binary inclusion control problem was proposed in [12].

In distributed control of MASs, real-time data transmission and processing underpin inter-agent information exchange and cooperative decision-making. However, constrained communication bandwidth, limited computational resources, and low-power design requirements impose urgent demands for efficient representation of input signals. As a core solution, input quantization maps continuously valued input signals into discrete values with finite bit-width, significantly reducing communication loads and computational complexity. Yet, this process inevitably introduces quantization errors, posing challenges to cooperative accuracy, stability, and convergence performance. Consequently, scholars have achieved notable advancements in addressing these issues through quantizer design, stability assurance mechanisms, and intelligent compensation strategies [13-16]. In [17], for a class of non-strict feedback high-order nonlinear systems with input quantization, an adaptive fuzzy predefined-time tracking control scheme is proposed. In [18], the problem of adaptive stabilization is explored for stochastic systems with input delay, where both the states and the input are quantized. For a class of strict-feedback nonlinear

systems featuring input quantization, input delay, and prescribed performance, an adaptive optimal control method grounded in the command filter technique is put forward in [19].

In modern complex engineering systems such as industrial control systems, aerospace, and autonomous driving, sensors serve as critical components for system state perception, whose reliability directly determines system safety and operational performance. However, factors including harsh working environments, component aging, or sudden disturbances may cause sensor faults such as deviations, drifts, jamming, or complete failures, leading to distorted measurement information, which consequently triggers control strategy failures or even system breakdowns. Therefore, the development of advanced fault-tolerant control methods capable of handling sensor failures has become a pivotal technical challenge to ensure reliable system operation and has garnered significant research achievements [20-23]. In [24], the authors proposed an adaptive finite-time fault-tolerant observer-based quantized controller for nonlinear state-delayed interconnected switched multi-input multi-output systems. For vehicle platoons addressing sensor faults and output quantization, a fault-tolerant control scheme was established in [25]. In [26], a decentralized adaptive fault-tolerant control scheme for interconnected nonlinear systems with unknown multiplicative/time-varying additive sensor faults and uncertain cross-subsystem interactions was proposed. In [27], the problem of event-triggered fault-tolerant tracking control was studied for multi-agent systems with sensor/actuator faults.

Based on the above analysis, this paper investigates the adaptive containment control problem for nonlinear multi-agent systems with input quantization and sensor faults. The main contributions are summarized as follows:

- 1) For nonlinear multi-agent systems subject to dual effects of sensor faults and input quantization, an adaptive containment control scheme is proposed. By designing a distributed fuzzy adaptive control strategy, it ensures that the outputs of all followers converge to the convex hull formed by multiple leaders.
- 2) Combining a state observer with fuzzy logic systems, unmeasurable states are estimated, and uncertain nonlinear dynamics of the system are approximated. By constructing an absolute cubic Lyapunov function, the impact of sensor faults on control performance is effectively compensated. Additionally, a filter is introduced to reduce computational complexity in the recursive design of the backstepping approach.
- 3) Multi-parameter adaptive laws are proposed to dynamically adjust estimates of uncertain dynamic parameters, fault coefficients, and filter error compensation terms. Based on stability theory, the practical fixed-time stability of the closed-loop system is rigorously proven, and the effectiveness of the proposed scheme is validated through numerical simulations.

The subsequent sections of this paper are organized as below. Section 2 introduces the preliminaries and the dynamic model of the systems. An observer is designed and an adaptive quantized fault-tolerant control scheme is proposed in Section 3. Section 4 conducts a stability analysis. A simulation example is given in Section 5. Lastly, Section 6 summarizes the conclusions.

2. Preliminaries and Problem Statements

This section introduces graph theory, radial basis function neural networks (RBFNNs), key lemmas, and system dynamics.

2.1 Graph Theory

Let $\mathcal{G} = (\mathcal{V}, \mathcal{S}, \mathcal{A})$ be a directed graph, describing the interaction relationships among multiple agents. Here $\mathcal{V} = \{1, \dots, N + M\}$ denotes the node set, where followers are labeled as $i = \{1, \dots, N\}$, and leaders are labeled as $i = \{N + 1, \dots, N + M\}$. $\mathcal{S} \subseteq \mathcal{V} \times \mathcal{V}$ as the edge set. The weighted adjacency matrix is defined as

$\mathcal{A} = [a_{ij}] \in \mathbb{R}^{(N+M) \times (N+M)}$. If $(j, i) \in \mathcal{S}$, then $a_{ij} > 0$, indicating that agent i can receive information from agent

j , otherwise, $a_{ij} = 0$, with the assumption that $a_{ii} = 0$. The degree matrix is defined as $\mathcal{D} = \text{diag}(b_1, \dots, b_{N+M})$,

where $b_i = \sum_{j=1, j \neq i}^{N+M} a_{ij}$. The Laplacian matrix of the directed graph is given by $\mathcal{L} = \mathcal{D} - \mathcal{A} = [\ell_{ij}] \in \mathbb{R}^{(N+M) \times (N+M)}$,

where $\ell_{ii} = \sum_{j \neq i} a_{ij}$, $\ell_{ij} = -a_{ij}, i \neq j$.

Define the neighbor set of agent i as $\mathcal{N}_i = \{j | (j, i) \in \mathcal{E}\}$, and assume that $\mathcal{N}_i \neq \emptyset$ for $i = 1, \dots, N$, while

$\mathcal{N}_i = \emptyset$ for $i = N + 1, \dots, N + M$. Under this configuration, the Laplacian matrix \mathcal{L} can be partitioned as

$$\mathcal{L} = \begin{bmatrix} \mathcal{L}_1 & \mathcal{L}_2 \\ 0_{M \times N} & 0_{M \times M} \end{bmatrix},$$

where $\mathcal{L}_1 \in R^{N \times N}$, $\mathcal{L}_2 \in R^{N \times M}$.

Form the definition of Laplacian matrix \mathcal{L} , one has $e_1 = \mathcal{L}_1 y + \mathcal{L}_2 y^d$, where $e_1 = [e_{11}, e_{21}, \dots, e_{N1}]^T$, $y = [y_1, y_2, \dots, y_N]^T$ and $y^d = [y_{N+1}^d, y_{N+2}^d, \dots, y_{N+M}^d]^T$. Let $y^r = [y_1^r, y_2^r, \dots, y_N^r]^T = -\mathcal{L}_1^{-1} \mathcal{L}_2 y^d$. Then, $e_1 = \mathcal{L}_1 (y - y^r)$. Thus,

$$\|y\|^2 \leq \frac{2\|e_1\|^2}{\underline{\sigma}^2(\mathcal{L}_1)} + \frac{2\|\mathcal{L}_2 y^d\|^2}{\underline{\sigma}^2(\mathcal{L}_1)}. \tag{1}$$

Assumption 2.1: The leader signals $y_i^d(t)$, $i = N + 1, \dots, N + M$, and all their derivatives are continuous and bounded.

Assumption 2.2: For every follower, there exists at least one directed path from a leader to that follower.

2.2 RBFNN

The radial basis function neural network (RBFNN) is used to approximate a continuous function $g(X)$ defined on a compact set Ω_X .

Let $g(X)$ be a continuous function on the compact set Ω_X . For an approximation error $\sigma > 0$ satisfying $|\sigma| \leq \bar{\sigma}$, where $\bar{\sigma} > 0$ is a constant, we have

$$g(x) = U^T \phi(X) + \sigma,$$

where $X = [X_1, \dots, X_r]^T$ is the input vector of the RBFNN, $\phi(X) = [\phi_1(X), \dots, \phi_m(X)]^T$ is the basis function vector, and

m denotes the number of nodes in the RBFNN. The ideal weight vector $U^* \in R_m$ is defined as

$$U^* = \arg \min_{U \in \mathbb{R}^m} \{ \sup_{X \in \Omega_X} |g(X) - U^T \phi(X)| \},$$

where $U = [U_1, U_2, \dots, U_m]^T$ represents the weight vector.

The basis function $\phi_i(X)$ is typically chosen as a Gaussian function:

$$\phi_i(X) = \exp\left[-\frac{(X - k_i)^T (X - k_i)}{l_i^2}\right],$$

where k_i and l_i , ($i=1, \dots, m$) the center and width of the Gaussian function, respectively.

Assumption 2.2: σ is bounded, i.e., $|\sigma| \leq \bar{\sigma}$, where $\bar{\sigma} > 0$ is a constant.

2.3 Needed Lemmas

Lemma 2.1[29]: For any $v > 0$ and $\zeta \in \mathbb{R}$, one has

$$0 \leq |\zeta| - \zeta \tanh\left(\frac{\zeta}{\epsilon}\right) \leq \bar{\epsilon}\epsilon,$$

where $\bar{\epsilon} = 0.2785$.

Lemma 2.2[30]: For $\forall x, y \in \mathbb{R}$, $\tau > 0$, $a > 0$ and $b > 0$ satisfying $(a-1)(b-1) = 1$, one has

$$xy \leq \frac{\tau^a}{a} |x|^a + \frac{1}{b\tau^b} |y|^b.$$

Lemma 2.3[31]: Let $V(t)$ be continuous and satisfy $V(t) > 0$. If $\dot{V}(t) \leq -aV(t) + \Delta$, where a and b are positive constants, one has

$$V(t) \leq V(0)e^{-at} + \frac{\Delta}{a}(1 - e^{-at}).$$

2.4 System Description

Consider a multi-agent system with M leaders and N followers, where the dynamic behavior of the followers is described as:

$$\begin{cases} \dot{\zeta}_{iq} = \zeta_{i,q+1} + g_{iq}(\underline{\zeta}_{iq}) + r_{iq}, q = 1, \dots, n-1, \\ \dot{\zeta}_{in} = Q(u_i) + g_{in}(\zeta_i) + r_{in}, \\ y_i = \zeta_{i1}, i = 1, \dots, N, \end{cases} \quad (2)$$

where $\zeta_{iq} \in \mathbb{R}$ denotes the system state, and $y_i \in \mathbb{R}$ represents the system output, where only $y_i = \zeta_{i1}$ is

directly measurable. The unknown smooth nonlinear function $g_{iq}(\cdot): \mathbb{R}^p \rightarrow \mathbb{R}$ is defined with $\underline{\zeta}_{iq} = [\zeta_{i1}, \dots, \zeta_{iq}]^T$

and $\zeta_i = [\zeta_{i1}, \dots, \zeta_{in}]^T$. The external disturbance $r_{iq} \in \mathbb{R}$ is unknown but bounded, satisfying $|r_{iq}| \leq \bar{r}_{iq}$, where

$\bar{r}_{iq} > 0$ is a constant. The control input $u_i \in \mathbb{R}$ is converted into a quantized input $Q(u_i)$, with the quantization error constrained by a sector-bounded condition:

$$|Q(u_i) - u_i| \leq \rho |u_i| + (1 - \rho)d, \quad (3)$$

where $0 < \rho < 1$ and $d > 0$ are unknown constants.

Regarding the system output y_i , when a sensor failure occurs at time T_i^F , the measured output $y_i^F(t)$ is modeled as:

$$y_i^F(t) = \begin{cases} y_i(t), t \leq T_i^F, \\ \varpi_i y_i(t), t > T_i^F, \end{cases} \tag{4}$$

where $0 < \varpi_i < 1$ is an unknown fault parameter. Let $\tilde{\omega}_i = \omega_i - \hat{\omega}_i$, in which $\omega_i = \varpi_i^{-1}$ and $\hat{\omega}_i$ is the estimation of ω_i , which will be updated by an adaptive law.

Assumption 2.3: For the leader signal $y_d(t)$, $y_d^{(q)}$, $q = 1, 2, \dots, n$, are continuous and bounded.

3. State Observer Design

A state observer is constructed as:

$$\begin{cases} \dot{\hat{\zeta}}_{iq} = \hat{\zeta}_{i,q+1} + k_{iq}(\hat{\omega}_i y_i^F - \hat{y}_i), q = 1, \dots, n-1, \\ \dot{\hat{\zeta}}_{in} = Q(u_i) + k_{in}(\hat{\omega}_i y_i^F - \hat{y}_i), \\ \hat{y}_i = \hat{\zeta}_{i1} \end{cases} \tag{5}$$

where $\hat{\zeta}_{iq}$, $q = 1, \dots, n$, is the estimate of ζ_{iq} , and $k_{iq} > 0$ is a design parameter.

Define the observer error as $\tilde{\zeta}_{iq} = \zeta_{iq} - \hat{\zeta}_{iq}$, we have

$$\dot{\tilde{\zeta}}_i = A_i \tilde{\zeta}_i + G_i + r_i - K_i(\hat{\omega}_i y_i^F - y_i), \tag{6}$$

where $\tilde{\zeta}_i = \begin{bmatrix} \tilde{\zeta}_{i1} \\ \tilde{\zeta}_{i2} \\ \vdots \\ \tilde{\zeta}_{in} \end{bmatrix}$, $G_i = \begin{bmatrix} g_{i1}(\zeta_{i1}) \\ g_{i2}(\zeta_{i2}) \\ \vdots \\ g_{in}(\zeta_{in}) \end{bmatrix}$, $r_i = \begin{bmatrix} r_{i1} \\ r_{i2} \\ \vdots \\ r_{in} \end{bmatrix}$, $K_i = \begin{bmatrix} k_{i1} \\ k_{i2} \\ \vdots \\ k_{in} \end{bmatrix}$, $A_i = \begin{bmatrix} -k_{i1} & 1 & \dots & 0 \\ \vdots & \vdots & \ddots & \vdots \\ -k_{i,n-1} & 0 & \dots & 1 \\ -k_{in} & 0 & \dots & 0 \end{bmatrix}$. A_i is the

Hurwitz matrix, i.e., for the given Q_i there exists a positive-definite matrix P_i such that $A_i^T P_i + P_i A_i = -Q_i$.

Let

$$e_{i1} = \sum_{j=1}^N a_{ij}(y_i - y_j) + \sum_{j=N+1}^{N+M} a_{ij}(y_i - y_j^d), \tag{7}$$

$$e_{iq} = \zeta_{iq} - \alpha_{i,q-1}, \tag{8}$$

where $\alpha_{i,q-1}$, $q = 2, \dots, n$, is the virtual controller.

The Lyapunov function V_0 is defined as

$$V_0 = \sum_{i=1}^N \tilde{\zeta}_i^T P_i \tilde{\zeta}_i. \tag{9}$$

From (6) and (9), one has

$$\begin{aligned} \dot{V}_0 &= 2 \sum_{i=1}^N \tilde{\zeta}_i^T P_i \dot{\tilde{\zeta}}_i \\ &= 2 \sum_{i=1}^N \tilde{\zeta}_i^T P_i [A_i \tilde{\zeta}_i + G_i + r_i - K_i (\hat{\omega}_i y_i^F - y_i)] \\ &= \sum_{i=1}^N [-\tilde{\zeta}_i^T Q_i \tilde{\zeta}_i + 2 \tilde{\zeta}_i^T P_i (G_i + r_i) - 2 \tilde{\zeta}_i^T P_i K_i (\hat{\omega}_i y_i^F - y_i)]. \end{aligned} \tag{10}$$

From (4) and Young’s inequality, one has

$$\begin{aligned} -\sum_{i=1}^N 2 \tilde{\zeta}_i^T P_i K_i (\hat{\omega}_i y_i^F - y_i) &= \sum_{i=1}^N 2 \tilde{\zeta}_i^T P_i K_i \tilde{\omega}_i y_i^F \\ &\leq \sum_{i=1}^N [\tau_i \|P_i K_i\|^2 \|\tilde{\zeta}_i\|^2 + \frac{1}{\tau_i} \tilde{\omega}_i^2 (y_i^F)^2] \end{aligned} \tag{11}$$

and

$$2 \tilde{\zeta}_i^T P_i (G_i + r_i) \leq \|\tilde{\zeta}_i\|^2 + 2 \|P_i\|^2 \|G_i\|^2 + 2 \|P_i\|^2 \bar{r}_i^2, \tag{12}$$

where $\tau_i > 0$ is a constant and $\bar{r}_i = [\bar{r}_{i1}, \dots, \bar{r}_{in}]^T$.

For the unknown nonlinear term $\|G_i\|^2$ in (3.8), an RBFNN $U_{i0}^T \phi_{i0}$ is applied such that $\|G_i\|^2 = U_{i0}^T \phi_{i0} + \sigma_{i0}$,

where σ_{i0} is the approximation error with $|\sigma_{i0}| \leq \bar{\sigma}_{i0}$. Based on the fact that $0 < \phi_{i0}^T \phi_{i0} \leq 1$, we have

$$\|G_i\|^2 \leq \|U_{i0}\| \|\phi_{i0}\| + |\sigma_{i0}| \leq \theta_{i0} + \bar{\sigma}_{i0},$$

where $\theta_{i0} = \|U_{i0}\|$. Thus, one has

$$2 \tilde{\zeta}_i^T P_i (G_i + r_i) \leq \|\tilde{\zeta}_i\|^2 + 2 \|P_i\|^2 (\theta_{i0} + \bar{\sigma}_{i0}) + 2 \|P_i\|^2 \bar{r}_i^2. \tag{13}$$

Substituting (11) and (13) into (10), we have

$$\dot{V}_0 = \sum_{i=1}^N [-\alpha_i^{(0)} \|\tilde{\zeta}_i\|^2 + \Delta_i^{(0)} + \frac{1}{\tau_i} \tilde{\omega}_i^2 (y_i^F)^2], \tag{14}$$

where $r_i^{(0)} = \lambda_{\min}(Q_i) - 1 - \tau_i \|P_i K_i\|^2$ and $\Delta_i^{(0)} = 2 \|P_i\|^2 (\theta_{i0} + \bar{\sigma}_{i0}) + 2 \|P_i\|^2 \bar{r}_i^2$.

4. Adaptive Controller Design

Let θ_{iq} denote an unknown constant, to be defined subsequently. $\hat{\theta}_{iq}$ represents the estimate of θ_{iq} . Define the estimation error as $\tilde{\theta}_{iq} = \theta_{iq} - \hat{\theta}_{iq}$.

Step 1: From (2) and (7), one has

$$\begin{aligned} \dot{e}_{i1} &= \sum_{j=1}^{N+M} a_{ij} \dot{y}_i - \sum_{j=1}^N a_{ij} \dot{y}_j - \sum_{j=N+1}^{N+M} a_{ij} \dot{y}_j^d \\ &= b_i (e_{i2} + \alpha_{i1} + g_{i1}(\zeta_{i1}) + r_{i1}) - \sum_{j=1}^N a_{ij} (\zeta_{j2} + f_{j1}(\zeta_{j1}) + r_{j1}) - \sum_{j=N+1}^{N+M} a_{ij} \dot{y}_j^d, \end{aligned} \tag{15}$$

where $b_i = \sum_{j=1}^{N+M} a_{ij}$.

Define the Lyapunov function V_1 as follows

$$V_1 = V_0 + \sum_{i=1}^N V_{i1} = V_0 + \sum_{i=1}^N \left(\frac{1}{2} e_{i1}^2 + \frac{1}{2\mu_{i1}} \tilde{\theta}_{i1}^2 + \frac{1}{3} |\tilde{\omega}_i|^3 \right), \tag{16}$$

where μ_{i1} is positive constant.

From (15) and (16), one has

$$\begin{aligned} \dot{V}_{i1} &= e_{i1} \dot{e}_{i1} - \frac{1}{\mu_{i1}} \tilde{\theta}_{i1} \dot{\tilde{\theta}}_{i1} + \tilde{\omega}_i^2 \dot{\tilde{\omega}}_i \text{sgn}(\tilde{\omega}_i) \\ &= e_{i1} [b_i (e_{i2} + \alpha_{i1} + g_{i1}(\zeta_{i1}) + r_{i1}) - \sum_{j=1}^N a_{ij} (\zeta_{j2} + g_{j1}(\zeta_{j1}) + r_{j1}) \\ &\quad - \sum_{j=N+1}^{N+M} a_{ij} \dot{y}_j^d] - \frac{1}{\mu_{i1}} \tilde{\theta}_{i1} \dot{\tilde{\theta}}_{i1} + \tilde{\omega}_i^2 \dot{\tilde{\omega}}_i \text{sgn}(\tilde{\omega}_i). \end{aligned} \tag{17}$$

Using Young's inequality, one has

$$b_i e_{i1} (e_{i2} + r_{i1}) \leq b_i^2 e_{i1}^2 + \frac{1}{2} e_{i2}^2 + \frac{1}{2} \bar{r}_{i1}^2 \tag{18}$$

and

$$-e_{i1} \sum_{j=1}^N a_{ij} r_{j1} \leq \frac{1}{2} \sum_{j=1}^N a_{ij} e_{i1}^2 + \frac{1}{2} \sum_{j=1}^N a_{ij} \bar{r}_{j1}^2. \tag{19}$$

Let

$$G_{i1} = (b_i^2 + \frac{1}{2} \sum_{j=1}^N a_{ij}) e_{i1} + b_i g_{i1}(\zeta_{i1}) - \sum_{j=1}^N a_{ij} (\zeta_{j2} + g_{j1}(\zeta_{j1})) - \sum_{j=N+1}^{N+M} a_{ij} \dot{y}_j^d. \tag{20}$$

The function G_{i1} is approximated by a RBFNN $U_{i1}^T \phi_{i1}$, i.e., $G_{i1} = U_{i1}^T \phi_{i1} + \sigma_{i1}$, where σ_{i1} is the estimation error satisfying $|\sigma_{i1}| \leq \bar{\sigma}_{i1}$ with $\bar{\sigma}_{i1} > 0$. Thus, we have

$$\begin{aligned} e_{i1} G_{i1} &= e_{i1} (U_{i1}^T \phi_{i1} + \sigma_{i1}) \\ &\leq |e_{i1}| (\|U_{i1}\| \|\phi_{i1}\| + |\sigma_{i1}|) \\ &\leq |e_{i1}| (\theta_{i1} + \bar{\sigma}_{i1}) \\ &\leq \theta_{i1} e_{i1} \tanh\left(\frac{e_{i1}}{\epsilon_{i1}}\right) + \theta_{i1} \bar{\epsilon}_{i1} + \frac{1}{2} e_{i1}^2 + \frac{1}{2} \bar{\sigma}_{i1}^2, \end{aligned} \tag{21}$$

where $\theta_{i1} = \|U_{i1}\|$ and $\epsilon_{i1} > 0$ is a constant.

Select the virtual controller α_{i1} as

$$\alpha_{i1} = \frac{1}{b_i} \left(-p_{i1} e_{i1} - \frac{1}{2} e_{i1} - \hat{\theta}_{i1} \tanh\left(\frac{e_{i1}}{\epsilon_{i1}}\right) \right), \tag{22}$$

where $p_{i1} > 0$ is a design parameter. The adaptive laws $\dot{\hat{\theta}}_{i1}$ and $\dot{\hat{\omega}}_i$ is designed as

$$\dot{\hat{\theta}}_{i1} = -\eta_{i1} \hat{\theta}_{i1} + \mu_{i1} e_{i1} \tanh\left(\frac{e_{i1}}{\epsilon_{i1}}\right), \tag{23}$$

and

$$\dot{\hat{\omega}}_i = \begin{cases} \frac{1}{\tau_i} (y_i^F)^2 - \xi_i \hat{\omega}_i, & \frac{1}{\tau_i} (y_i^F)^2 - \xi_i \hat{\omega}_i > 0, \\ 0, & \frac{1}{\tau_i} (y_i^F)^2 - \xi_i \hat{\omega}_i \leq 0, \end{cases} \tag{24}$$

where η_{i1} and ξ_i are positive constants.

Based on Lemma 2.2, we have

$$\tilde{\omega}_i^2 \hat{\omega}_i \text{sgn}(\tilde{\omega}_i) = \tilde{\omega}_i^2 \hat{\omega}_i \frac{|\tilde{\omega}_i|}{\tilde{\omega}_i} = (\omega_i - \tilde{\omega}_i) \tilde{\omega}_i \left(|\tilde{\omega}_i| \leq \omega_i \right) |\tilde{\omega}_i|^2 - |\tilde{\omega}_i|^3 \leq -\frac{1}{3} |\tilde{\omega}_i|^3 + \frac{1}{3} \omega_i^3. \tag{25}$$

From (16)-(25), one has

$$\dot{V}_1 \leq \sum_{i=1}^N (-a_i^{(0)} \|\tilde{\zeta}_i\|^2 + \Delta_i^{(1)} - p_{i1} e_{i1}^2 + \frac{1}{2} e_{i2}^2 + \frac{\eta_{i1}}{\mu_{i1}} \tilde{\theta}_{i1} \hat{\theta}_{i1}^2 - \frac{\xi_i}{3} |\tilde{\omega}_i|^3), \tag{26}$$

where $\Delta_i^{(1)} = \Delta_i^{(0)} + \frac{1}{2} \bar{r}_{i1}^2 + \frac{1}{2} \sum_{j=1}^N a_{ij} \bar{r}_{j1}^2 + \theta_{i1} \bar{\epsilon}_{i1} + \frac{1}{2} \bar{\sigma}_{i1}^2 + \frac{\xi_i}{3} \omega_i^3$.

Step q ($q = 2, \dots, n-1$): From (2) and (8), one has

$$\begin{aligned} \dot{e}_{iq} &= \dot{\zeta}_{iq} - \dot{\alpha}_{i,q-1} \\ &= e_{i,q+1} + \alpha_{iq} + g_{iq}(\underline{\zeta}_{iq}) + r_{iq} - \dot{\alpha}_{i,q-1}. \end{aligned} \tag{27}$$

Using the following second-order differentiator [32] to approximate $\dot{\alpha}_{i,q-1}$

$$\begin{cases} \dot{h}_{iq} = \hat{h}_{iq}, \\ \dot{\hat{h}}_{iq} = -\frac{1}{j^2} [\text{sat}(\text{sgn}(H(h_{iq} - \alpha_{iq}, j\hat{h}_{iq}))) |H(h_{iq} - \alpha_{iq}, j\hat{h}_{iq})|^{2-p}) + \text{sat}(\text{sgn}(\hat{h}_{iq}) |j\hat{h}_{iq}|^p)], \end{cases} \tag{28}$$

where

$$H(h_{iq} - \alpha_{iq}, j\hat{h}_{iq}) = h_{iq} - \alpha_{iq} + \frac{\text{sgn}(\hat{h}_{iq}) |j\hat{h}_{iq}|^{2-p}}{2-p}, \tag{29}$$

$$\text{sat}(x) = \begin{cases} x, & |x| < P, \\ P \text{sgn}(x), & |x| \geq P, \end{cases} \tag{30}$$

$\text{sgn}(\cdot)$ denotes the sign function, $j > 0$, $P > 0$, $p \in (0, 1)$ are design parameters, and differentiator states

h_{iq} and \hat{h}_{iq} are the estimations of $\alpha_{i,q-1}$ and $\dot{\alpha}_{i,q-1}$, respectively.

Therefore, the derivative of $\alpha_{i,q-1}$ is expressed as

$$\dot{\alpha}_{i,q-1} = \hat{h}_{iq} + \kappa_{iq}, \tag{31}$$

where κ_{iq} denotes the estimated error of the differentiator. To address this error, a compensated filtering error mechanism is formulated

$$\kappa_{iq} = \hat{\kappa}_{iq} + \tilde{\kappa}_{iq}, \tag{32}$$

where $\hat{\kappa}_{iq}$ represents the approximated filtering error, and $\tilde{\kappa}_{iq}$ corresponds to the residual compensation error.

The Lyapunov function candidate V_q is selected as:

$$V_q = V_{q-1} + \sum_{i=1}^N V_{iq} = V_{q-1} + \sum_{i=1}^N \left(\frac{1}{2} e_{iq}^2 + \frac{1}{2\mu_{iq}} \tilde{\theta}_{iq}^2 + \frac{1}{2\gamma_{iq}} \tilde{\kappa}_{iq}^2 \right), \tag{33}$$

where μ_{iq} and γ_{iq} are positive constants.

Form (27)-(33), we have

$$\begin{aligned} \dot{V}_{iq} &= e_{iq} \dot{e}_{iq} - \frac{1}{\mu_{iq}} \tilde{\theta}_{iq} \dot{\tilde{\theta}}_{iq} - \frac{1}{\gamma_{iq}} \tilde{\kappa}_{iq} \dot{\tilde{\kappa}}_{iq} \\ &= e_{iq} (e_{i,q+1} + \alpha_{iq} + g_{iq}(\underline{\zeta}_{iq}) + r_{iq} - \dot{h}_{iq} - \dot{\hat{\kappa}}_{iq} - \dot{\tilde{\kappa}}_{iq}) - \frac{1}{\mu_{iq}} \tilde{\theta}_{iq} \dot{\tilde{\theta}}_{iq} - \frac{1}{\gamma_{iq}} \tilde{\kappa}_{iq} \dot{\tilde{\kappa}}_{iq}. \end{aligned} \tag{34}$$

Similar to (18), we have

$$e_{iq} (e_{i,q+1} + r_{iq}) \leq e_{iq}^2 + \frac{1}{2} e_{i,q+1}^2 + \frac{1}{2} r_{iq}^2. \tag{35}$$

Let

$$G_{iq} = \frac{3}{2} e_{iq} + g_{iq}(\underline{\zeta}_{iq}). \tag{36}$$

Similar to (21), G_{iq} is approximated by a RBFNN $U_{iq}^T \phi_{iq}$, i.e., $G_{iq} = U_{iq}^T \phi_{iq} + \sigma_{iq}$, where σ_{iq} is the estimation

error satisfying $|\sigma_{iq}| \leq \bar{\sigma}_{iq}$ with $\bar{\sigma}_{iq} > 0$. One has

$$\begin{aligned} e_{iq} G_{iq} &= e_{iq} (U_{iq}^T \phi_{iq} + \sigma_{iq}) \\ &\leq e_{iq} (\|U_{iq}\| \|\phi_{iq}\| + |\sigma_{iq}|) \\ &\leq e_{iq} (\theta_{iq} + \bar{\sigma}_{iq}) \\ &\leq \theta_{iq} e_{iq} \tanh\left(\frac{e_{iq}}{\epsilon_{iq}}\right) + \theta_{iq} \bar{\epsilon}_{iq} + \frac{1}{2} e_{iq}^2 + \frac{1}{2} \bar{\sigma}_{iq}^2, \end{aligned} \tag{37}$$

where ϵ_{iq} is a positive constant and $\theta_{iq} = \|U_{iq}\|$.

The virtual control law α_{iq} is designed as:

$$\alpha_{iq} = -p_{iq}e_{iq} - \frac{1}{2}e_{iq} - \hat{\theta}_{iq} \tanh\left(\frac{e_{iq}}{\epsilon_{iq}}\right) + \hat{h}_{iq} + \hat{\kappa}_{iq}, \tag{38}$$

where p_{iq} is a positive constant.

The adaptive laws $\hat{\theta}_{iq}$ and $\hat{\kappa}_{iq}$ are designed as

$$\dot{\hat{\theta}}_{iq} = -\eta_{iq}\hat{\theta} + \mu_{iq}e_{iq} \tanh\left(\frac{e_{iq}}{\epsilon_{iq}}\right) \tag{39}$$

and

$$\dot{\hat{\kappa}}_{iq} = -\beta_{iq}\hat{\kappa}_{iq} - \gamma_{iq}e_{iq}, \tag{40}$$

where η_{iq} and β_{iq} are positive constants.

Taking (35)-(40) into (34), we have

$$\dot{V}_q \leq \sum_{i=1}^N \{-a_i^{(0)}\|\tilde{\zeta}_i\|^2 + \Delta_i^{(q)} - \sum_{l=1}^q p_{il}e_{il}^2 + \frac{1}{2}e_{i,q+1}^2 + \sum_{l=1}^q \frac{\eta_{il}}{\mu_{il}}\tilde{\theta}_{il}\hat{\theta}_{il} + \sum_{l=2}^q \frac{\beta_{il}}{\gamma_{il}}\tilde{\kappa}_{il}\hat{\kappa}_{il} - \frac{\xi_i}{3}|\tilde{\omega}_i|^3\}, \tag{41}$$

where $\Delta_i^{(p)} = \Delta_i^{(p-1)} + \frac{1}{2}\bar{r}_{iq}^2 + \theta_{iq}\bar{\epsilon}\epsilon_{iq} + \frac{1}{2}\bar{\sigma}_{iq}^2$.

Step n: From (2) and (8), we have

$$\dot{e}_{in} = \dot{\zeta}_{in} - \dot{\alpha}_{i,n-1} = Q(u_i) + g_{in}(\zeta_i) + r_{in} - \dot{\alpha}_{i,n-1}. \tag{42}$$

The Lyapunov function V_n is constructed as

$$V_n = V_{n-1} + \sum_{i=1}^N \left(\frac{1}{2}e_{in}^2 + \frac{1}{2\mu_{in}}\tilde{\theta}_{in}^2 + \frac{1}{2\gamma_{in}}\tilde{\kappa}_{in}^2\right), \tag{43}$$

where μ_{in} and γ_{in} are positive constants.

Combining equations (42) and (43), we have

$$\begin{aligned} \dot{V}_{in} &= e_{in}\dot{e}_{in} - \frac{1}{\mu_{in}}\tilde{\theta}_{in}\dot{\tilde{\theta}}_{in} - \frac{1}{\eta_{in}^{(3)}}\tilde{\sigma}_{in}\dot{\tilde{\sigma}}_{in} - \frac{1}{\gamma_{in}}\tilde{\kappa}_{in}\dot{\tilde{\kappa}}_{in} \\ &= e_{in}(Q(u_i) + g_{in}(\zeta_i) + r_{in} - \dot{h}_{in} - \dot{\kappa}_{in} - \tilde{\kappa}_{in}) - \frac{1}{\mu_{in}}\tilde{\theta}_{in}\dot{\tilde{\theta}}_{in} - \frac{1}{\gamma_{in}}\tilde{\kappa}_{in}\dot{\tilde{\kappa}}_{in}. \end{aligned} \tag{44}$$

Applying Young's inequality, one has

$$e_{in}r_{in} \leq \frac{1}{2}e_{in}^2 + \frac{1}{2}\bar{r}_{in}^2. \tag{45}$$

The actual control input u_i and adaptive laws are designed as follows

$$u_i = -p_{in}e_{in} - \frac{1}{2}e_{in} - \hat{\theta}_{in} \tanh\left(\frac{e_{in}}{\epsilon_{in}^{(1)}}\right) + \hat{h}_{in} + \hat{\kappa}_{in}, \tag{46}$$

$$\dot{\hat{\theta}}_{in} = -\eta_{in}\hat{\theta}_{in} + \mu_{in}e_{in} \tanh\left(\frac{e_{in}}{\epsilon_{in}^{(1)}}\right), \tag{47}$$

and

$$\dot{\hat{\kappa}}_{in} = -\beta_{in}\hat{\kappa}_{in} - \gamma_{in}e_{in}, \tag{48}$$

where p_{in} , $\epsilon_{in}^{(1)}$, η_{in} , and β_{in} are positive constants.

Integrating (3) and (46), one has

$$\begin{aligned} e_{in}Q(u_i) &\leq e_{in}u_i + |e_{in}|[\rho|u_i| + (1-\rho)d] \\ &\leq e_{in}u_i + |e_{in}|[\rho(p_{in}|e_{in}| + \frac{1}{2}|e_{in}| + |\hat{\theta}_{in}| + |\hat{h}_{in}| + |\hat{\kappa}_{in}|) + (1-\rho)d] \\ &\leq e_{in}u_i + \rho p_{in}e_{in}^2 + \frac{1}{2}\rho e_{in}^2 + \rho e_{in}\hat{\theta}_{in} \tanh(\frac{e_{in}\hat{\theta}_{in}}{\epsilon_{in}^{(2)}}) + \rho e_{in}\hat{h}_{in} \tanh(\frac{e_{in}\hat{h}_{in}}{\epsilon_{in}^{(3)}}) + \rho e_{in}\hat{\kappa}_{in} \tanh(\frac{e_{in}\hat{\kappa}_{in}}{\epsilon_{in}^{(4)}}) \\ &\quad + (1-\rho)d e_{in} \tanh(\frac{e_{in}}{\epsilon_{in}^{(5)}}) + \rho\bar{\epsilon}(\epsilon_{in}^{(2)} + \epsilon_{in}^{(3)} + \epsilon_{in}^{(4)}) + (1-\rho)d\bar{\epsilon}\epsilon_{in}^{(5)}, \end{aligned} \tag{49}$$

where $\epsilon_{in}^{(l)}$, $l = 2, \dots, 5$, are positive constants.

Let

$$\begin{aligned} G_{in} &= e_{in} + \rho p_{in}e_{in} + \frac{1}{2}\rho e_{in} + g_{in}(\zeta_i) + \rho\hat{\theta}_{in} \tanh(\frac{e_{in}\hat{\theta}_{in}}{\epsilon_{in}^{(2)}}) + \rho\hat{h}_{in} \tanh(\frac{e_{in}\hat{h}_{in}}{\epsilon_{in}^{(3)}}) \\ &\quad + \rho\hat{\kappa}_{in} \tanh(\frac{e_{in}\hat{\kappa}_{in}}{\epsilon_{in}^{(4)}}) + (1-\rho)d \tanh(\frac{e_{in}}{\epsilon_{in}^{(5)}}). \end{aligned} \tag{50}$$

Similar to (21), one has

$$\begin{aligned} e_{in}G_{in} &= e_{in}(U_{in}^T\phi_{in} + \sigma_{in}) \\ &\leq |e_{in}|(\|U_{in}\| \|\phi_{in}\| + |\sigma_{in}|) \\ &\leq |e_{in}|(\theta_{in} + \bar{\sigma}_{in}) \\ &\leq \theta_{in}e_{in} \tanh(\frac{e_{in}}{\epsilon_{in}^{(1)}}) + \theta_{in}\bar{\epsilon}\epsilon_{in}^{(1)} + \frac{1}{2}e_{in}^2 + \frac{1}{2}\bar{\sigma}_{in}^2, \end{aligned} \tag{51}$$

where $\theta_{in} = \|U_{in}\|$.

From (43)-(51), we have

$$\dot{V}_n \leq \sum_{i=1}^N (-a_i^{(n)}\zeta_i^T P_i \zeta_i + \Delta_i^{(n)} - \sum_{l=1}^n p_{il}e_{il}^2 + \sum_{l=1}^n \eta_{il}\tilde{\theta}_{il}\hat{\theta}_{il} + \sum_{l=2}^n \beta_{il}\tilde{\kappa}_{il}\hat{\kappa}_{il} - \frac{\xi_i}{3}|\tilde{\omega}_i|^3), \tag{52}$$

where $a_i^{(n)} = a_i^{(0)} / \lambda_{\max}(P_i) > 0$, and $\Delta_i^{(n)} = \Delta_i^{(n-1)} + \frac{1}{2}\bar{r}_{in}^2 + \theta_{in}\bar{\epsilon}\epsilon_{in}^{(1)} + \frac{1}{2}\bar{\sigma}_{in}^2 + \rho\bar{\epsilon}(\epsilon_{in}^{(2)} + \epsilon_{in}^{(3)} + \epsilon_{in}^{(4)}) + (1-\rho)d\bar{\epsilon}\epsilon_{in}^{(5)}$.

5. Stability Analysis

Theorem 5.1: Under Assumptions 2.1-2.3, consider the nonlinear multi-agent system (2) with input quantization and sensor faults. By integrating the state observer (5), controllers (22), (38), (46), adaptive laws (23), (24), (39), (40), (47), (48), along with the second-order filter (28), the following control objectives are rigorously guaranteed:

- 1) The error signals $\tilde{\zeta}_{iq}$, e_{iq} , $\tilde{\theta}_{iq}$, $\tilde{\omega}_i$, $\tilde{\kappa}_{iq}$ remain globally uniformly bounded. Furthermore, these errors

satisfy

$$\|\tilde{\zeta}_i\| \leq \sqrt{\frac{\Delta}{a\lambda_{\min}(P_i)}}, \tag{53}$$

$$|e_{il}| \leq \sqrt{\frac{2\Delta}{a}}, l=1, \dots, n, \tag{54}$$

$$|\tilde{\theta}_{il}| \leq \sqrt{\frac{2\mu_{il}\Delta}{a}}, l=1, \dots, n, \tag{55}$$

$$|\tilde{\omega}_i| \leq \sqrt[3]{\frac{3\Delta}{a}}, \tag{56}$$

and

$$|\tilde{\kappa}_{il}| \leq \sqrt{\frac{2\gamma_{il}\Delta}{a}}, l=2, \dots, n. \tag{57}$$

2) The containment error is bounded.

Proof: From (9), (16), (33), and (43), we have

$$V_n = \sum_{i=1}^N (\tilde{\zeta}_i^T P_i \tilde{\zeta}_i + \sum_{l=1}^n \frac{1}{2} e_{il}^2 + \sum_{l=1}^n \frac{1}{2\mu_{il}} \tilde{\theta}_{il}^2 + \sum_{l=2}^n \frac{1}{2\gamma_{il}} \tilde{\kappa}_{il}^2 + \frac{1}{3} |\tilde{\omega}_i|^3), \tag{58}$$

By using Young's inequality, one has

$$\frac{\eta_{il}}{\mu_{il}} \tilde{\theta}_{il} \hat{\theta}_{il} = \frac{\eta_{il}}{\mu_{il}} (\tilde{\theta}_{il} \theta_{il} - \tilde{\theta}_{il}^2) \leq \frac{\eta_{il}}{2\mu_{il}} (\theta_{il}^2 - \tilde{\theta}_{il}^2), \tag{59}$$

and

$$\frac{\beta_{il}}{\gamma_{il}} \tilde{\kappa}_{il} \hat{\kappa}_{il} = \frac{\beta_{il}}{\gamma_{il}} (\tilde{\kappa}_{il} \kappa_{il} - \tilde{\kappa}_{il}^2) \leq \frac{\beta_{il}}{2\gamma_{il}} (\kappa_{il}^2 - \tilde{\kappa}_{il}^2). \tag{60}$$

Substituting (59) and (60) into (52), one has

$$\dot{V}_n \leq -\sum_{i=1}^N (a_i^{(n)} \tilde{\zeta}_i^T P_i \tilde{\zeta}_i + \sum_{l=1}^n p_{il} e_{il}^2 + \sum_{l=1}^n \frac{\eta_{il}}{2\mu_{il}} \tilde{\theta}_{il}^2 + \sum_{l=2}^n \frac{\beta_{il}}{2\gamma_{il}} \tilde{\kappa}_{il}^2 - \frac{\xi_i}{3} |\tilde{\omega}_i|^3 + \Delta_i), \tag{61}$$

where $\Delta_i = \Delta_i^{(n)} + \sum_{l=1}^n \frac{\eta_{il}}{2\mu_{il}} \theta_{il}^2 + \sum_{l=2}^n \frac{\beta_{il}}{2\gamma_{il}} \kappa_{il}^2$.

Let $p_i = \min_{1 \leq l \leq n} 2p_{il}$, $\eta_i = \min_{1 \leq l \leq n} \eta_{il}$ and $\beta_i = \min_{2 \leq l \leq n} \beta_{il}$, one has

$$\begin{aligned} \dot{V}_n &\leq -\sum_{i=1}^N (a_i^{(n)} \tilde{\zeta}_i^T P_i \tilde{\zeta}_i + p_i \sum_{l=1}^n \frac{e_{il}^2}{2} + \eta_i \sum_{l=1}^n \frac{1}{2\mu_{il}} \tilde{\theta}_{il}^2 + \beta_i \sum_{l=2}^n \frac{1}{2\gamma_{il}} \tilde{\kappa}_{il}^2 - \frac{\xi_i}{3} |\tilde{\omega}_i|^3 + \Delta_i) \\ &\leq -\sum_{i=1}^N a_i (\tilde{\zeta}_i^T P_i \tilde{\zeta}_i + \sum_{l=1}^n \frac{e_{il}^2}{2} + \sum_{l=1}^n \frac{1}{2\mu_{il}} \tilde{\theta}_{il}^2 + \sum_{l=2}^n \frac{1}{2\gamma_{il}} \tilde{\kappa}_{il}^2 - \frac{1}{3} |\tilde{\omega}_i|^3 + \Delta_i) \\ &\leq -a \sum_{i=1}^N (\tilde{\zeta}_i^T P_i \tilde{\zeta}_i + \sum_{l=1}^n \frac{e_{il}^2}{2} + \sum_{l=1}^n \frac{1}{2\mu_{il}} \tilde{\theta}_{il}^2 + \sum_{l=2}^n \frac{1}{2\gamma_{il}} \tilde{\kappa}_{il}^2 - \frac{1}{3} |\tilde{\omega}_i|^3) + \Delta \\ &= aV_n + \Delta, \end{aligned} \tag{62}$$

where $a_i = \min\{a^{(n)}, p_i, \eta_i, \beta_i, \xi_i\}$, $a = \min_{1 \leq i \leq N} a_i$, $\Delta = \sum_{i=1}^N \Delta_i$.

From (62) and Lemma 2.3, one has

$$0 \leq V_n \leq \frac{\Delta}{a} + (V_n(0) - \frac{\Delta}{a})e^{-at}. \tag{63}$$

Thus,

$$V_n \leq \frac{\Delta}{a}, t \rightarrow \infty. \tag{64}$$

1) From (58) and (64), one has

$$\tilde{\zeta}_i^T P_i \tilde{\zeta}_i \leq V_n \leq \frac{\Delta}{a},$$

thus,

$$\|\tilde{\zeta}_i\| \leq \sqrt{\frac{\Delta}{a\lambda_{\min}(P_i)}}.$$

Similarly, (54)-(57) hold.

2) Defining the containment error as $e = y - y^r$, one has

$$\|e\| = \|y - y^r\| \leq \|y\| + \|\mathcal{L}_1^{-1} \mathcal{L}_2\| \|y^d\|. \tag{65}$$

By (1) and Assumption 2.1, the containment error is bounded.

Proof completed.

6. Numerical Simulation

Consider a nonlinear multi-agent system comprising four followers and two leaders, with the connectivity graph depicted in Figure 1. The dynamics of the followers are described by:

$$\begin{cases} \dot{\zeta}_{i1} = \zeta_{i2} + \zeta_{i1} \sin(0.5\zeta_{i1}) + 0.5 \sin(0.3t), \\ \dot{\zeta}_{i2} = Q(u_i) + \zeta_{i2} \sin(0.5\zeta_{i1}\zeta_{i2}) + 0.2 \sin(0.5t), \\ y_i = \zeta_{i1}, i = 1, \dots, 4. \end{cases}$$

And the two leader signals are respectively set as $y_5^d = \sin(0.35t) + 1$, $y_6^d = \sin(0.35t) - 1$. Under sensor faults, the system output model is defined as:

$$y_i^F(t) = \begin{cases} y_i(t), t \leq T_i^F, \\ 0.85y_i(t), t > T_i^F, \end{cases}$$

with fault occurrence times $T_1^F = 20s$, $T_2^F = 20s$, $T_3^F = 10s$, and $T_4^F = 10s$. The input signal is quantized using the hysteresis quantizer model [33], with the parameter configuration being $\rho = 0.1$, $d = 0.08$.

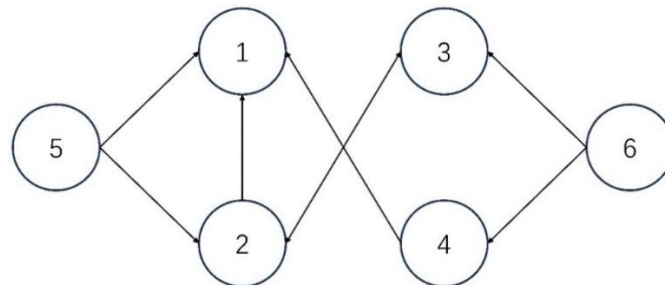


Figure 1. Adirectedgraph

For each unknown function, the RBFNN comprises 5 nodes. The centers of the Gaussian functions are uniformly selected within the interval $[-2, 2]$, and their width is set to 2. The main parameters are selected as $k_{11} = 9$, $k_{12} = 5.4$, $k_{21} = 6.8$, $k_{22} = 5.35$, $k_{31} = 20$, $k_{32} = 9$, $k_{41} = 15$, $k_{42} = 8$, $p_{11} = 45$, $p_{12} = 20$, $p_{21} = 60$, $p_{22} = 25$, $p_{31} = 60$, $p_{32} = 25$, $p_{41} = 45$, $p_{42} = 20$, $\eta_{i1} = 2$, $\eta_{i2} = 5$, $\mu_{i1} = 1$, $\mu_{i2} = 0.5$, $\beta_{i2} = 0.3$, $\gamma_{i2} = 40$, $\xi_i = 1$, $\tau_1 = 0.85$, $\tau_2 = 1.03$, $\tau_3 = 1.03$, $\tau_4 = 1.62$, $j = 0.04$, $P = 1$, $p = 0.5$.

The simulation results are shown in Figures 2 to 4-9. Figure 2 illustrates the trajectories of the system outputs ζ_{iq} , $i = 1, \dots, 4$, $q = 1, 2$, and leader signals y_i^d , $i = 5, 6$. Figure 3 depicts the observer error $\tilde{\zeta}_i$, $i = 1, \dots, 4$, which remains confined within a small neighborhood around zero, exhibiting only transient oscillations after fault occurrences. Figure 4 presents the control signals u_i , $i = 1, \dots, 4$ and their quantization signals $Q(u_i)$. The curves of adaptive laws $\hat{\theta}_q$, $\hat{\omega}_i$ and $\hat{\kappa}_{i2}$ for $i = 1, \dots, 4$, $q = 1, 2$ are shown in Figures 5-7, respectively. The results demonstrate that under the proposed adaptive control scheme, all followers converge into the convex hull formed by the leaders while ensuring boundedness of all closed-loop system signals.

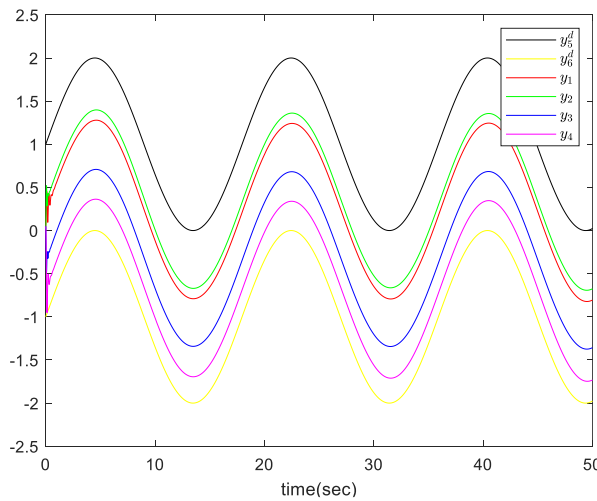


Figure 2. The curves of $y_i (i = 1, \dots, 4)$ and $y_i^d (i = 5, 6)$

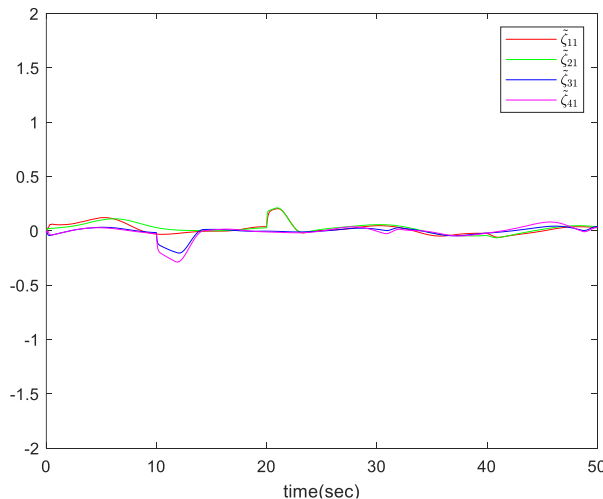


Figure 3. The curves of $\tilde{\zeta}_i (i = 1, \dots, 4)$

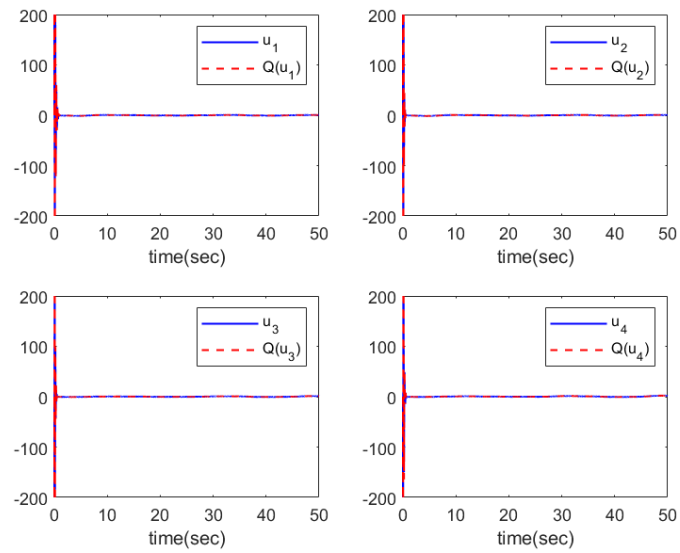


Figure 4. The curves of u_i and $Q(u_i)(i=1, \dots, 4)$

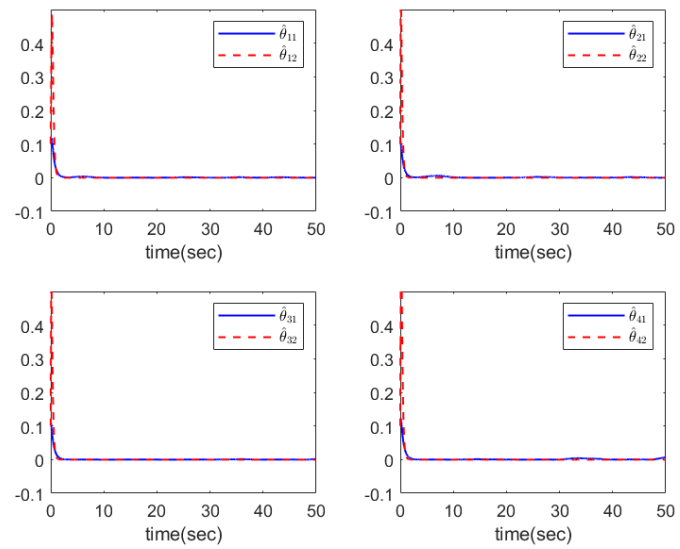


Figure 5. The curves of $\hat{\theta}_{ij}(i=1, \dots, 4, j=1, 2)$

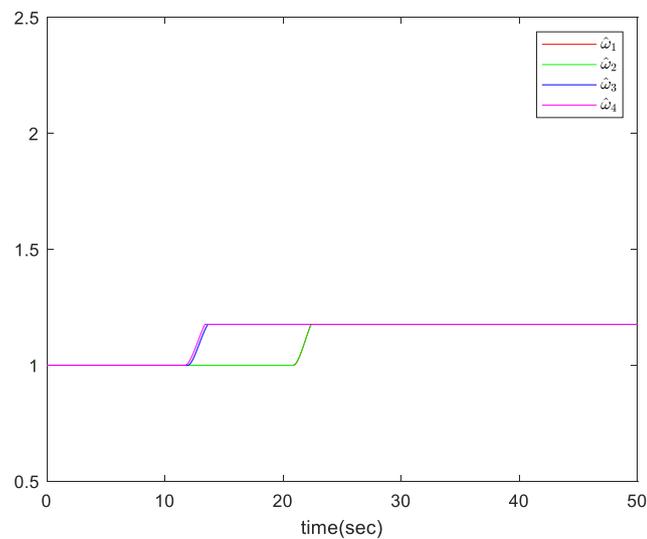


Figure 6. The curves of $\hat{\omega}_i(i=1, \dots, 4)$

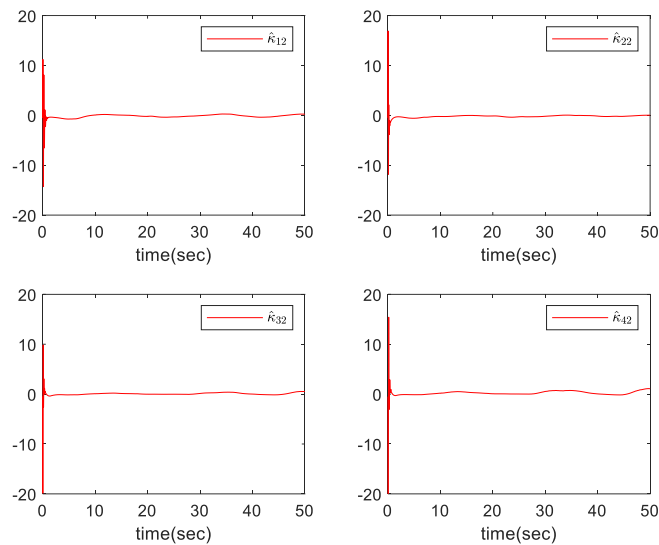


Figure 7. The curves of $\hat{\kappa}_{i2} (i=1, \dots, 4)$

7. Conclusion

This paper proposes an adaptive containment control scheme for nonlinear multi-agent systems coexisting with sensor faults and input quantization. By integrating a state observer, a RBFNN, and a second-order filter, the scheme achieves the estimation of unmeasurable states, the approximation of uncertain dynamics, and the reduction of computational complexity. An absolute cubic Lyapunov function is constructed, which is combined with a multi-parameter adaptive law design, to compensate for the interference of sensor faults on system performance and ensure that all followers converge to the convex hull formed by leaders within a fixed time. The practical fixed-time stability of the closed-loop system is rigorously proven through stability analysis, and numerical simulations further validate the effectiveness of the proposed approach.

References

- [1] Wang, L., Wang, K., Pan, C., et al. (2021). Multi-agent deep reinforcement learning-based trajectory planning for multi-UAV assisted mobile edge computing. *IEEE Transactions on Cognitive Communications and Networking*, 7(1), 73–84. <https://doi.org/10.1109/TCCN.2020.3027695>
- [2] Yang, J., Zhang, J., & Wang, H. (2021). Urban traffic control in software defined internet of things via a multi-agent deep reinforcement learning approach. *IEEE Transactions on Intelligent Transportation Systems*, 22(6), 3742–3754. <https://doi.org/10.1109/TITS.2020.3023788>
- [3] Parrany, A. M., & Alasty, A. (2025). Decentralized leader-following control of a heterogeneous swarm robotic system subject to network-induced imperfections. *Unmanned Systems*, 13(01), 69–90. <https://doi.org/10.1142/S2301385025500050>
- [4] Cai, J., Wu, W., Yi, C., et al. (2025). Neural adaptive dynamic event-triggered containment control for uncertain multi-agent systems under Markovian switching dynamics. *Cognitive Computation*, 17(1), 1–14. <https://doi.org/10.1007/s12559-024-10388-9>
- [5] Habibi, H., Iftekhhar, L., Rahman, M. H., et al. (2025). Cooperative learning-based practical formation-containment control with prescribed performance for heterogeneous clusters of UAV/USV. *Asian Journal of Control*, 27(2), 921–947. <https://doi.org/10.1002/asjc.3480>
- [6] Wang, H., & Li, M. (2025). Adaptive fuzzy nonsingular fixed-time safety flight containment control for multi-UAVs. *IEEE Transactions on Aerospace and Electronic Systems*, 61(1), 802–812. <https://doi.org/10.1109/TAES.2024.3448398>
- [7] Zhang, T., Zhang, S., Li, H., et al. (2025). Velocity-free prescribed-time orbit containment control for satellite clusters under actuator saturation. *Advances in Space Research*, 75(6), 5110–5123. <https://doi.org/10.1016/j.asr.2024.12.039>
- [8] Zhang, Z., Huang, B., Zhou, X., et al. (2025). Fully distributed dynamic event-triggered formation-containment

- control for networked unmanned surface vehicles with intermittent wireless network communications. *ISA Transactions*, 156, 202–216. <https://doi.org/10.1016/j.isatra.2024.10.033>
- [9] Wang, L., & Dong, J. (2022). Adaptive fuzzy consensus tracking control for uncertain fractional-order multiagent systems with event-triggered input. *IEEE Transactions on Fuzzy Systems*, 30(2), 310–320. <https://doi.org/10.1109/TFUZZ.2020.3037957>
- [10] Yao, D., Wu, Y., Ren, H., et al. (2025). Event-based adaptive sliding-mode containment control for multiple networked mechanical systems with parameter uncertainties. *IEEE Transactions on Automation Science and Engineering*, 22, 264–275. <https://doi.org/10.1109/TASE.2024.3349634>
- [11] Wang, L., Yan, H., Hu, X., et al. (2025). Fixed-time bipartite containment control for heterogeneous multiagent systems under DoS attacks: An event-triggered mechanism. *IEEE Transactions on Systems, Man, and Cybernetics: Systems*, 55(4), 2782–2794. <https://doi.org/10.1109/TSMC.2024.3523705>
- [12] Ba, D., Li, Y., & Tong, S. (2019). Fixed-time adaptive neural tracking control for a class of uncertain nonstrict nonlinear systems. *Neurocomputing*, 363, 273–280. <https://doi.org/10.1016/j.neucom.2019.06.063>
- [13] Ning, J., Wang, Y., Wang, E., et al. (2025). Fuzzy trajectory tracking control of under-actuated unmanned surface vehicles with ocean current and input quantization. *IEEE Transactions on Systems, Man, and Cybernetics: Systems*, 55(1), 63–72. <https://doi.org/10.1109/TSMC.2024.3460370>
- [14] Li, H., & Li, M. (2025). A dynamic gain method to event-triggered tracking control for uncertain nonlinear systems with input quantization. *IEEE Transactions on Automatic Control*, 1–8. <https://doi.org/10.1109/TAC.2025.3545551>
- [15] Yang, Y., Sui, S., Liu, T., et al. (2025). Adaptive predefined time control for stochastic switched nonlinear systems with full-state error constraints and input quantization. *IEEE Transactions on Cybernetics*, 1–12. <https://doi.org/10.1109/TCYB.2025.3555205>
- [16] Cheng, W., Cheng, H., Wang, F., et al. (2025). Fixed-time neural consensus control for nonlinear multiagent systems with state and input quantization. *Chaos, Solitons & Fractals*, 194, 116145. <https://doi.org/10.1016/j.chaos.2025.116145>
- [17] Sui, S., Zhao, L., & Chen, C. P. (2024). Adaptive fuzzy predefined-time tracking control design for nonstrict-feedback high-order nonlinear systems with input quantization. *IEEE Transactions on Fuzzy Systems*, 32(10), 5978–5990. <https://doi.org/10.1109/TFUZZ.2024.3431047>
- [18] Wu, J., Yang, Y., Chen, W., et al. (2025). Adaptive neural fault tolerant control for input-delayed stochastic systems subject to states and input quantization. *IEEE Transactions on Systems, Man, and Cybernetics: Systems*, 55(4), 2451–2462. <https://doi.org/10.1109/TSMC.2025.3525508>
- [19] Xia, X., Li, C., Zhang, T., et al. (2025). Adaptive prescribed performance optimal control for strict-feedback nonlinear systems with input delay and input quantization. *Journal of the Franklin Institute*, 362(4), 107568. <https://doi.org/10.1016/j.jfranklin.2025.107568>
- [20] Qin, L., He, X., Yan, R., et al. (2017). Active fault-tolerant control for a quadrotor with sensor faults. *Journal of Intelligent & Robotic Systems*, 88, 449–467. <https://doi.org/10.1007/s10846-017-0474-0>
- [21] Nadi, A., Mahzoon, M., & Azadi Yazdi, E. (2025). Adaptive fault tolerant control for cantilever thick plates with piezoelectric patches. *Scientific Reports*, 15(1), 388. <https://doi.org/10.1038/s41598-024-84420-1>
- [22] Ri, K. C., Kim, Y. I., & Ri, S. J. (2025). Robust fault-tolerant control and application in DCS with uncertainty and time delay. *International Journal of Dynamics and Control*, 13(2), 44. <https://doi.org/10.1007/s40435-024-01535-z>
- [23] Wu, T., Yu, Z., & Li, S. (2022). Observer-based adaptive fuzzy quantized fault-tolerant control of nonstrict-feedback nonlinear systems with sensor fault. *IEEE Transactions on Fuzzy Systems*, 31(6), 1900–1911. <https://doi.org/10.1109/TFUZZ.2022.3216113>
- [24] Ghoreishee, A., & Soroush, M. (2025). Adaptive fault-tolerant observer-based control for multi-input multi-output interconnected systems with bandwidth-limited communication. *Control Engineering Practice*, 156, 106217. <https://doi.org/10.1016/j.conengprac.2024.106217>
- [25] Liu, X., Yan, M., Yang, P., et al. (2024). Unknown input observer based neuro-adaptive fault-tolerant control for vehicle platoons with sensor fault and output quantization. *Control Engineering Practice*, 150, 106007. <https://doi.org/10.1016/j.conengprac.2024.106007>

- [26] Fang, X., Fan, H., Liu, L., et al. (2023). Decentralized adaptive fault-tolerant control of interconnected systems with sensor faults. *Journal of Control and Decision*, 12(2), 289–305. <https://doi.org/10.1080/23307706.2023.2227184>
- [27] Ye, Z., Yu, Z., Jiang, B., et al. (2025). Event-triggered fault-tolerant tracking control for multiagent systems under actuator/sensor faults. *ISA Transactions*, 156, 30–38. <https://doi.org/10.1016/j.isatra.2024.11.012>
- [28] Lv, W., Lu, J., Li, Y., et al. (2022). Adaptive neural finite-time control of nonlinear systems subject to sensor hysteresis. *Journal of the Franklin Institute*, 359(7), 2932–2948. <https://doi.org/10.1016/j.jfranklin.2022.02.032>
- [29] Polycarpou, M. M., & Ioannou, P. A. (1996). A robust adaptive nonlinear control design. *Automatica*, 32(3), 423–427. [https://doi.org/10.1016/0005-1098\(95\)00147-6](https://doi.org/10.1016/0005-1098(95)00147-6)
- [30] Deng, H., & Krstić, M. (1997). Stochastic nonlinear stabilization—I: A backstepping design. *Systems & Control Letters*, 32(3), 143–150. [https://doi.org/10.1016/S0167-6911\(97\)00068-6](https://doi.org/10.1016/S0167-6911(97)00068-6)
- [31] Hou, Z., Cheng, L., & Tan, M. (2009). Decentralized robust adaptive control for the multiagent system consensus problem using neural networks. *IEEE Transactions on Systems, Man, and Cybernetics, Part B (Cybernetics)*, 39(3), 636–647. <https://doi.org/10.1109/TSMCB.2008.2007810>
- [32] Wang, X., Chen, Z., & Yang, G. (2007). Finite-time-convergent differentiator based on singular perturbation technique. *IEEE Transactions on Automatic Control*, 52(9), 1731–1737. <https://doi.org/10.1109/TAC.2007.904290>
- [33] Xing, L., Wen, C., Zhu, Y., et al. (2016). Output feedback control for uncertain nonlinear systems with input quantization. *Automatica*, 65, 191–202. <https://doi.org/10.1016/j.automatica.2015.11.028>

Copyrights

Copyright for this article is retained by the author(s), with first publication rights granted to the journal.

This is an open-access article distributed under the terms and conditions of the Creative Commons Attribution license (<http://creativecommons.org/licenses/by/4.0/>).